Interaction of Poly(methacrylic acid) Brushes with Metal Ions: An Infrared Investigation

Rupert Konradi and Jürgen Rühe*

Institute for Microsystem Technology, University of Freiburg, D-79110 Freiburg, Germany

Received May 4, 2004; Revised Manuscript Received June 9, 2004

ABSTRACT: The complexation of poly(methacrylic acid) (PMAA) brushes prepared by the "grafting from" technique with silver, calcium, copper, aluminum, and lanthanum ions was studied. XP and IR spectra confirmed the formation of stable complexes. The IR spectra revealed different coordination geometries depending on the nature of the metal ion. The degree of complex formation was strongly dependent on both the metal ion concentration and the graft density of the polymer brush. The degree of dissociation of the PMAA brush and the total amount of calcium adsorbed were quantitatively evaluated.

1. Introduction

The interaction of polycarboxylates with metal cations is of outstanding importance in biology and in numerous technological applications. For instance, polycarboxylates are widely used as superabsorbing materials,[1] for wastewater treatment,[2] for the dispersion of inorganic solids in water,[3] and for the production of ultrafine, high surface area, high reactivity ceramic oxide powders.[4] Most interesting, however, is the fact that polycarboxylates are ubiquitous in biology given that proteins contain carboxylic acid moieties. The interaction of Ca^{2+} and COO^- groups of proteins and the concomitant change in the swelling of the biopolymer is a crucial step in the clotting of blood, nerve excitation, muscle contraction, and cell locomotion.[5,6]

When linear polymer chains are anchored with one end to a surface and the anchoring distance between two chains is less than the radius of gyration of the same polymer chain in solution, segment−segment repulsion will lead to a stretching of the polymer chains, and a so-called polymer brush conformation is adopted. Polymer brushes have been the subject of numerous theoretical investigations since the late 1970s.[7−10] Only recently, also detailed experimental studies were carried out. Brushes have been synthesized via phase separation in the Langmuir trough,[11,12] physisorption of block copolymers or end-functionalized polymers,[13,14] and chemisorption of either preformed polymer molecules (macroinitiators)[15] or self-assembled monolayers of initiator molecules that are used in a subsequent step to grow polymer chains at the surface of the substrate in situ.[16−18] The last approach has been termed "grafting from" polymerization in contrast to the adsorption of preformed polymer molecules ("grafting to") and was also employed in the present study. The "grafting from" technique has two major advantages over the other techniques: First, the polymer molecules are covalently linked to the surface and therefore inherently more stable than physisorbed layers. Second, a much higher graft density can be achieved in comparison to the "grafting to" method where adsorption is kinetically hindered.[19,20] Upon the introduction of charges along the polymer chain, one enters the interesting field of polyelectrolyte brushes. Potential applications of these systems for colloid stabilization,[21] (bio)lubrication,[22] and (bio)sensor[23] devices have been reported. With respect to polyelectrolyte brushes, one has to distinguish between so-called strong or quenched polyelectrolyte brushes where the charge density along the chain is fixed and weak or annealed polyelectrolyte brushes where the charge density can be tuned externally, e.g., via the pH value of the surrounding solution.[24−27] Strong polyelectrolyte brushes have been synthesized in one- or two-step approaches and examined with respect to their swelling behavior in solutions of varying ionic strength.[28,29] Detailed aspects of the synthesis and characterization of polyelectrolyte brushes have been recently reviewed.[23,30,31] First experimental investigations on the properties of weak polyelectrolyte brushes have now been published.[32,33] However, still very little is known about specific interactions of these brushes with monovalent and especially with multivalent cations. In theoretical treatments, these interactions were often neglected, and only ionic interactions were taken into consideration.[34,35] In this article, we report on the complexation of PMAA brushes with silver, calcium, copper, aluminum, and lanthanum ions. We discuss the influence of the chemical nature, valency, and concentration of these ions and the influence of the graft density of the brush.

2. Experimental Section

2.1. Materials. Silicon wafers (CrysTec, Germany), 750 μm thick, were polished on both faces and had an oxide layer of approximately 2 nm. They were cleaned with a stream of high-velocity dry ice particles (Tectra, Germany) prior to the immobilization to remove dust particles. Methacrylic acid (Fluka, Germany) was purified by vacuum distillation over a Vigreux column and stored under nitrogen at −20 °C. Water was deionized with a Millipore system (resistivity ≥ 18.2 MΩ cm^{-1}) immediately prior to use.

2.2. Instrumentation. Transmission Fourier transform infrared (FTIR) spectra were recorded using a Bio-Rad Excalibur spectrometer over a frequency range from 4000 to 400 cm^{-1} with a resolution of 4 cm^{-1}. Typically, 128 scans were accumulated. The sample compartment was carefully purged with nitrogen to reduce water−OH and carbon dioxide absorption bands from the gas phase. Especially the water−OH bands in the carbonyl absorption region limit the sensitivity of transmission measurements. In practice, silicon wafers with polymer layers of thicknesses down to approximately 2 × 20 nm could be measured.

* Corresponding author. E-mail ruehe@imtek.uni-freiburg.de.

10.1021/ma049126x CCC: $27.50
Published on Web 08/05/2004

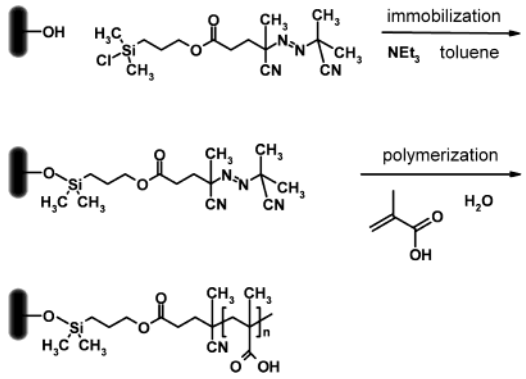

Figure 1. Schematic depiction of the "grafting from" free radical polymerization, using a self-assembled layer of azo initiators.

To determine the dry layer thicknesses, null ellipsometry and X-ray reflectometry (XRR) measurements were performed. Null ellipsometric measurements were carried out at an incident angle of 70° on an ELX-2 ellipsometer (Riss, Germany). The light source was a He−Ne laser with a wavelength of 632.8 nm and an intensity of 3 mW.

XRR data were obtained on a Bruker AXS D5000 instrument. An X-ray beam with a wavelength of 0.154 nm ($K\alpha_1$) was generated from a 40 kW, 20 mA cermanic anode with a copper target. The maximum thickness which could be resolved was 228 nm at an angular resolution of 0.001°.

XPS measurements were carried out on a Perkin-Elmer PHI 5600 spectrometer using Mg Kα radiation. The step width during accumulation of the spectra was set to 0.8 eV for survey and 0.1−0.13 eV for detail scans. The respective pass energies were 187.85 and 11.75−58.70 eV. The analyzer was positioned at 45° relative to the substrate surface.

2.3. Synthesis of the PMAA Brushes. PMAA brushes were synthesized via a surface-initiated free radical chain polymerization ("grafting from") as depicted in Figure 1. The procedure was described in detail by Prucker and Rühe.[16−18] In the first step a self-assembled monolayer of an azo initiator was formed on the surface of silicon wafers. The initiator molecules were covalently attached via a monochlorosilane functionality. In a second step, the surface-bound azo moiety was used to thermally initiate the polymerization of methacrylic acid. Reaction mixtures had a concentration of 10 vol % methacrylic acid in water and were carefully degassed by repeated ultrasonication and the application of vacuum before the initiator-functionalized substrates were added under nitrogen. The polymerization reactions were carried out in a thermostat at 60.0 ± 0.1 °C. In such a free radical polymerization, the grafting density can be controlled by varying the conversion of the surface-attached initiator, which can be adjusted via the polymerization time. The molecular weight of the surface-attached polymer molecules can be independently controlled via the monomer concentration. After polymerization, the PMAA brushes were extracted in methanol and water for approximately 15 h.

2.4. Complexation of the PMAA Brushes with Metal Ions. PMAA brushes were brought into contact with solutions of silver, calcium, copper, aluminum, and lanthanum nitrate of different concentrations. The solutions were prepared from analytical grade salts and deionized water of a resistivity ≥18.2 MΩ cm^{-1}. The system was allowed to equilibrate for approximately 1 h. (IR spectra showed no change after an adsorption time of a few minutes.) Then the samples were carefully rinsed with deionized water and dried before acquisition of infrared and XP spectra.

3. Results and Discussion

3.1. Control of the Brush Thickness and the Graft Density. A series of PMAA brushes with different graft densities and a constant molecular weight were prepared as described in section 2.3. Figure 2b shows the dry thickness of these brushes as a function of the polymerization time as measured by ellipsometry and XRR. The corresponding XRR spectra and simulations are depicted in Figure 2a. The roughness of the polymer layers was 0.3 nm for layer thicknesses < ≈50 nm and up to 2 nm for the thickest layer measured by XRR (228 nm). The thickness could be adjusted between a few nanometers and more than 400 nm. The solid line in Figure 2b represents the graft density $\Gamma(t)$ as a function of the polymerization time as calculated on the basis of the known initiator decomposition kinetics:[16,17]

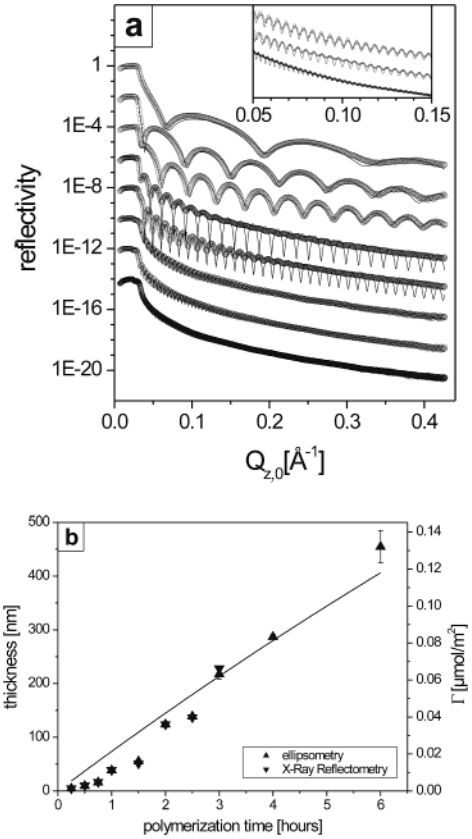

Figure 2. (a) XRR spectra for a series of PMAA brushes with different graft densities prepared by the "grafting from" method using different polymerization times. The solid lines represent simulations to obtain thicknesses and roughnesses of the polymer layers from the data. The spectra were offset by a factor of 100 for clarity. Polymerization times were 0.25, 0.5, 0.75, 1, 1.5, 2, 2.5, and 3 h, from top to bottom. The inset shows an enlargement for the last three polymerization times. (b) Brush thickness as a function of the polymerization time as determined by ellipsometry (▲) and XRR (▼). The solid line represents the graft density $\Gamma(t)$ as a function of the polymerization time as calculated according to eq 1.

$$\Gamma(t) = f\,\Gamma_0(1 - e^{-kt}) \qquad (1)$$

Here, Γ_0 is the graft density of the initiator and corresponds to the maximum graft density of the polymer brush in the case of a fully decomposed initiator and a theoretical radical efficiency f of 1. k is the rate constant of the initiator decomposition. The constants have been previously measured for the given initiator system and are $\Gamma_0 = 1.8 \pm 0.2$ μmol/m^2, $f = 0.35 \pm 0.05$, and $k = (9.6 \pm 1.0) \times 10^{-6}$ s^{-1}.[16,17] The graft density Γ can be related to the distance D between two anchoring points according to

$$D = (\Gamma N_A)^{-0.5} \qquad (2)$$

The measured thickness d of the polymer layer is connected to the graft density Γ through the molecular weight M_n and the density ρ of the polymer:

$$d = \frac{\Gamma M_n}{\rho} \tag{3}$$

with the bulk density $\rho = 1.12$ g/cm^3 of PMAA. As the number-averaged molecular weight M_n is independent of the polymerization time, one can derive M_n of the surface-attached polymer chains from a fit to the data with the only variable parameter M_n according to

$$d(t) = \frac{M_n}{\rho} f \Gamma_0 (1 - e^{-kt}) \tag{4}$$

M_n was found to be $(4 \pm 1) \times 10^6$ g/mol. The given error accounts for deviations at very short polymerization times which might stem from a slow heating of the Schlenk tubes in the thermostat. In principle, the molecular weight can be confirmed by GPC measurements. However, in this case, the molecular weight was not only much higher than any commercially available standard, but the higher molecular weight fraction of the polymer was also beyond the exclusion limit of the GPC columns. Therefore, the elugrams did not exactly represent the molecular weight distribution but in general confirm the outcome of the calculation above.

3.2. Formation of Metal Ion Complexes. The PMAA brushes were treated with different metal ions as described in section 2.4 to form polycarboxylate−metal ion complexes. Monovalent alkaline metal cations could not be used in this study since they do not form stable complexes with the polyacid and the dissociation equilibrium would be shifted upon rinsing the samples with deionized water. On the other hand, if no careful rinsing would be performed, the salt concentration would increase during drying of the sample, and significant amounts of salt would remain on the surface. All complexes with bivalent and multivalent cations were stable in water. Silver adsorption was partially reversible in water; however, the desorption was found to be slow. (An equilibrium was typically reached after 3−4 h.) After drying, the complexes were chemically characterized by XP spectroscopy. The expected elements were detected for all complexes. Figure 3a exemplarily shows the XP spectra (survey) of a PMAA brush before and after complexation with $Ca(NO_3)_2$. Figure 3b,c depicts the corresponding detail spectra. XP spectra could not be used for a quantitative analysis as poly(methacrylic acid) gradually decomposes upon exposure to X-rays.

3.3. Influence of the Nature of the Ion and the Ion Concentration. Typical transmission Fourier infrared (FTIR) spectra of a PMAA brush ($d = 2 \times 306$ nm, $\Gamma = 0.091$ μmol/m^2) after equilibration with water of pH 3 (top) and pH 12 (bottom) are presented in Figure 4. In the alkaline solution, the pH was adjusted with NaOH. At pH 3 (adjusted with HCl), the brush is in the protonated form and shows the characteristic poly(carboxylic acid) band peak at 1705 cm^{-1} (dashed line).[4,36] At pH 12, the brush is almost fully neutralized as confirmed by the asymmetric and symmetric stretching vibrations $\nu_{asym}(CO_2^-)$ and $\nu_{sym}(CO_2^-)$ of the carboxylate polyion at 1558 cm^{-1} (dashed line) and 1396 cm^{-1}, respectively.

Figure 5 shows the infrared spectra for a series of PMAA brushes ($d = 2 \times 316$ nm, $\Gamma = 0.091$ μmol/m^2) that were treated with increasing concentrations of (a) $AgNO_3$, (b) $Ca(NO_3)_2$, (c) $Cu(NO_3)_2$, (d) $Al(NO_3)_3$, and (e) $La(NO_3)_3$ at neutral pH. The concentrations were 10^{-5}, 10^{-4}, 10^{-3}, 10^{-2}, 10^{-1}, and 1 mol/L from top to bottom, respectively. The spectra at the bottom of the graph were taken after the samples were treated with diluted HCl of pH 2.5. At the lowest salt concentrations, all brushes were almost fully protonated. In the case of silver and calcium, the carboxylic acid vibrational band decreases with increasing ion concentration, and a concomitant increase of the carboxylate antisymmetric vibrational band was observed. This corresponds to a deprotonation of the polyacid due to an increasing complexation with the metal ions; i.e., protons are replaced by the metal ions. At ion concentrations $\geq 10^{-1}$ mol/L, the complexation with silver is stronger than with calcium although silver is only monovalent. Most remarkably, if one compares the two bivalent metal ions calcium and copper, it becomes evident that a third band is found in the carbonyl absorption band region at 1611 cm^{-1} for the PMAA brush copper ion complexes.

To understand the complex spectra of the different brushes, a comparison to the spectra of ion complexes

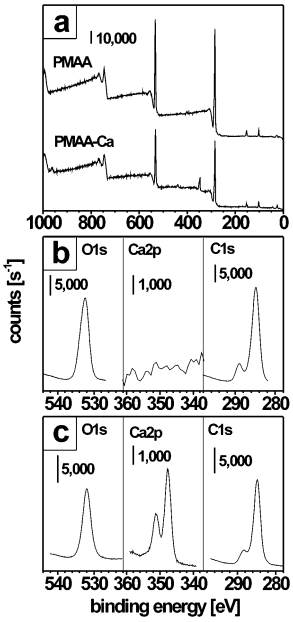

Figure 3. XP spectra of a PMAA brush before and after complexation with $Ca(NO_3)_2$. (a) shows the survey spectra; (b) and (c) show the corresponding detail spectra.

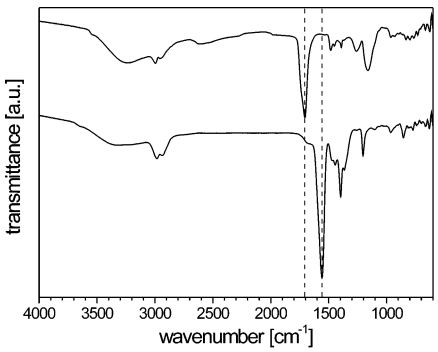

Figure 4. Transmission Fourier infrared (FTIR) spectra of a PMAA brush ($d = 2 \times 306$ nm, $\Gamma = 0.091$ μmol/m^2) after equilibration with water of pH 3 (top) and pH 12 (bottom). The dashed lines mark the characteristic absorption bands of the protonated and the deprotonated polyacid at 1705 and 1558 cm^{-1}, respectively.

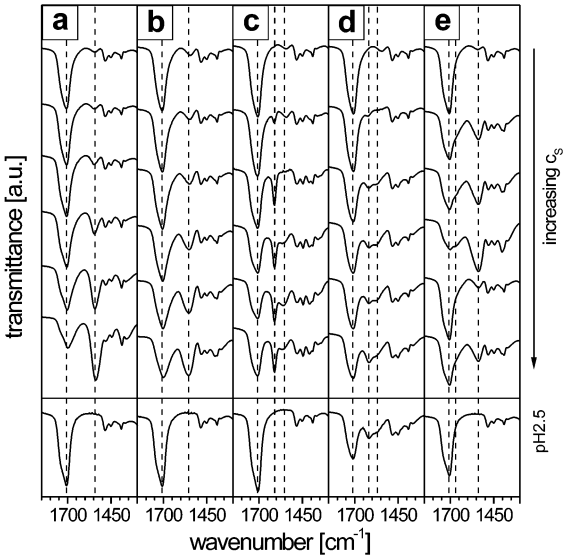

Figure 5. Transmission FTIR spectra (only the carbonyl absorption band region is shown) of a series of PMAA brushes ($d = 2 \times 316$ nm, $\Gamma = 0.091$ μmol/m^2) after complexation with metal ions of increasing concentration at neutral pH. Metal ions were (a) Ag^+, (b) Ca^{2+}, (c) Cu^{2+}, (d) Al^{3+}, and (e) La^{3+}. Concentrations were 10^{-5}, 10^{-4}, 10^{-3}, 10^{-2}, 10^{-1}, and 1 mol/L from top to bottom, respectively. The spectra at the bottom of the graph were taken after the samples were treated with diluted HCl of pH 2.5. Peaks corresponding to carboxylic acid and carboxylate vibrational bands are marked with a dashed line.

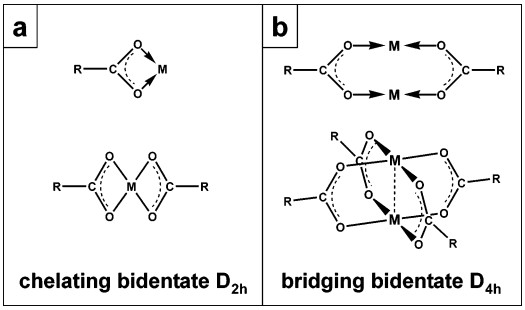

Figure 6. Schematical representation of the coordination of carboxylate ligands to metal ions: (a) chelating bidentate coordination; (b) bridging bidentate coordination. Charges are omitted for clarity.

of simple carboxylic acids and of poly(methacrylic acid) in solution can be made. Deacon and Phillips have reviewed acetate metal ion complexes and classified them according to the nature of carboxylate coordination.[37] Among a number of different coordination geometries that were observed, two are of particular significance: chelating bidentate and bridging bidentate. Both types of coordination involve a bidentate binding; i.e., both oxygen atoms of the carboxylate take part in the coordination. In the chelating coordination both oxygen atoms are bound to only one central ion, whereas in the bridging coordination the two oxygen atoms are bound to two different metal ions, essentially bridging the two. The chelating and bridging bidentate structures are schematically depicted in parts a and b of Figure 6, respectively. The different coordination geometries are reflected in differences in the carbonyl stretching frequencies. The corresponding absorption bands have been related to acetato complexes of known structure. For copper, both a mononuclear complex with a chelating bidentate acetate group, $Cu(O_2CCH_3)(Ph_3P)_2$, and a binuclear complex with bridging bidentate acetate groups, $[Cu(O_2CCH_3)_2(H_2O)]_2$, are known. The respective carbonyl absorption bands $\nu_{asym}(CO_2^-)$ were found at 1552 and 1610 cm^{-1}. The complexation of metal cations by polymeric carboxylic acids has also been investigated by infrared spectroscopy.[4] In these systems, often more than one band is found for the asymmetric carbonyl stretching vibration. McCluskey et al.[4] and others[38] have studied poly(acrylic acid) copper ion complexes and assigned the peaks at 1559 and at 1616 cm^{-1} to a chelating bidentate and a bridging bidentate coordination, respectively, in accordance with the data for the monomeric acetate complexes. When the carboxylate binds as a chelating bidentate ligand, mononuclear complexes with one or two carboxylates bound to the metal cation are formed. In the case of a bridging bidentate binding a binuclear complex is formed through the association of two copper ions with two pairs of adjacent carboxylate groups. In this dimer the copper ions are bridged by four carboxylate groups with two additional solvent ligands along the C_4 axis.

The spectra of the PMAA brush copper ion complexes in Figure 5c show bands corresponding to both a bridging bidentate ($\nu_{asym}(CO_2^-) = 1611$ cm^{-1}) and a chelating bidentate binding ($\nu_{asym}(CO_2^-) = 1558$ cm^{-1}). Hence, both coordination geometries coexist in the PMAA brush copper ion complex. However, the band at 1611 cm^{-1} emerges at lower ion concentrations in comparison to the one at 1557 cm^{-1}, indicating that the bridging complexation is stronger than the chelating complexation.

In the case of aluminum interacting with the PMAA brush (Figure 5d), also two carboxylate absorption bands at 1580 and 1616 cm^{-1} were found. The intensity of both peaks increases with increasing concentration. An absorption band at 1616 cm^{-1} in a poly(acrylic acid)−$Al(NO_3)_3$ adduct has again been assigned to a bridging bidentate conformation.[39] Peaks around 1575 cm^{-1} were usually assigned to be mainly ionic.[37,40]

Lanthanum ion PMAA brush complexes display a unique behavior (Figure 5e): First, the infrared spectra revealed an increase of the carboxylate band at 1539 cm^{-1} as expected. At 0.1 mol/L, however, the carboxylate peak intensity dramatically decreased with a concomitant increase of the carboxylic acid band. The carboxylate peak intensity did only slightly increase again at 1 mol/L. This behavior can be understood if one considers that hydrated lanthanum ions react acidic. The pH values of the solutions were 4.4 (0.1 mol/L) and 3.0 (1 mol/L) and were not adjusted to neutral pH as this would cause precipitation of lanthanum hydroxide. It is likely that the increase in the proton concentration with increasing lanthanum ion concentration is enough to establish a competitive coordination of protons with the carboxylate groups, effectively replacing lanthanum ions with protons. McCluskey et al.[4] have assigned the peak at 1543 cm^{-1} in a poly(acrylic acid) lanthanum ion complex to a chelating bidentate coordination and compared this to a rare earth acetate $[Eu(O_2CCH_3)_3(H_2O)_4]$ with a carboxylate peak at 1538 cm^{-1}. For this complex an arrangement involving chelating bidentate and monatomic bridging coordination has been reported.[37] To our knowledge, the shoulder around 1675 cm^{-1} has not been discussed up to now and seems to be unique for the polymer brush conformation. It is reasonable to assume that conformational constraints imposed by the brush during the lanthanum complexation alter

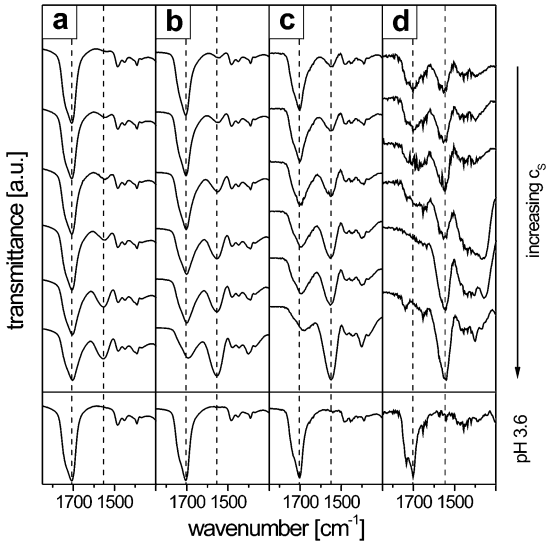

Figure 7. Transmission FTIR spectra (only the carbonyl absorption band region is shown) of four PMAA brushes of different graft densities after complexation with $Ca(NO_3)_2$ of increasing concentration at neutral pH. Graft densities Γ of the brushes were (a) 0.118 μmol/m^2 ($d = 2 \times 459$ nm), (b) 0.062 μmol/m^2 ($d = 2 \times 202$ nm), (c) 0.032 μmol/m^2 ($d = 2 \times 51$ nm), and (d) 0.016 μmol/m^2 ($d = 2 \times 17$ nm). Concentrations were 10^{-5}, 10^{-4}, 10^{-3}, 10^{-2}, 10^{-1}, and 1 mol/L from top to bottom, respectively. The spectra shown at the bottom of the graph were taken after the samples were treated with diluted HCl of pH 3.6. The wavenumbers which can be attributed to the carboxylic acid (1705 cm^{-1}) and the carboxylate (1555 cm^{-1}) vibrational bands are marked with a dashed line.

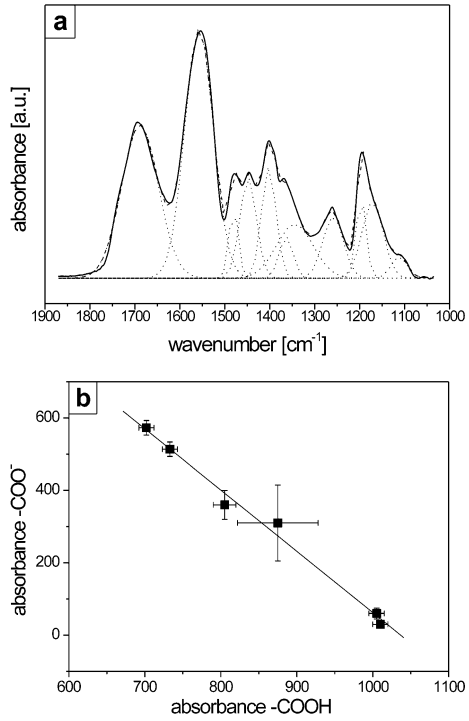

Figure 8. (a) Typical fit of an infrared absorption spectrum with multiple Gaussians. The solid line corresponds to the original data, the dotted lines represent individual peaks, and the calculated envelope is given by the dashed line. (b) Determination of the ratio of the extinction coefficients of the carboxylate and the carboxylic acid peak. The intensities for the two peaks were derived from spectra of the same brush at different calcium ion concentrations.

the typical dimeric structure of the carboxylic acid moieties to a certain extent, which would account for the shift in the peak position.

All samples were treated with diluted HCl of pH 2.5 after complexation in 1 mol/L solutions of the various salts in order to study the reversibility of the complex formation. The corresponding spectra recorded after this treatment can be found on the bottom of Figure 5, showing that the complexation was reversible under these conditions for all cations under investigation except for aluminum. This means that all metal ions except for aluminum could be replaced in their complexes with the PMAA brush by protons. The trivalent aluminum ion shows a much stronger bridging than the bivalent copper and the larger lanthanum ion. The fact that the latter one could be replaced with protons is in accordance with the observation that at high lanthanum concentrations, where the solution pH is low, the complexation was found to be almost reversed.

3.4. Quantitative Evaluation of the Infrared Spectra. To quantify the complexation of PMAA brushes with calcium in terms of the degree of dissociation α of the polyacid, infrared spectra at six calcium ion concentrations were evaluated for four brushes of different graft density. The spectra are shown in Figure 7. Again, the concentrations were 10^{-5}, 10^{-4}, 10^{-3}, 10^{-2}, 10^{-1}, and 1 mol/L from top to bottom, respectively, and the spectra shown at the bottom of the graph were taken after the samples were treated with diluted HCl of pH 3.6. The graft densities Γ of the brushes were (a) 0.118, (b) 0.062, (c) 0.032, and (d) 0.016 μmol/m^2, corresponding to anchoring distances D of (a) 3.7, (b) 5.1, (c) 7.1, and (d) 10 nm (eq 2).

The spectra were typically fit in the range from 1050 to 1850 cm^{-1} with up to 11 Gaussians. The relatively broad spectral range was chosen to ensure that the baselines for all spectra coincide. Note that no attempt was made to assign the peaks of wavenumbers lower than the respective carboxylate peak. However, the accurate peak areas in this region were important to allow for a precise determination of the integral of the carboxylate absorption band. A typical infrared absorption spectrum (solid line) with the corresponding fit is given in Figure 8a. Dotted lines describe the individual peaks, and the envelope is represented by the dashed line.

To calculate the number of carboxylic acid groups that were bound to calcium ions, one has to know the ratio of the extinction coefficients of the carboxylate and the carboxylic acid peak $\epsilon(COO^-)/\epsilon(COOH)$. With the assumption that the intensity loss in the carboxylic acid peak upon increasing complexation is reflected by the concomitant increase in the carboxylate peak intensity, one can expect that a plot of the carboxylate peak intensity vs the carboxylic acid peak intensity results in a linear function, the slope of which equals $\epsilon(COO^-)/\epsilon(COOH)$. Note that the total amount of carboxylate and carboxylic acid groups is fixed as the same PMAA brush was used for all concentrations. The corresponding plot is shown in Figure 8b. The $\epsilon(COO^-)/\epsilon(COOH)$ ratio was determined for all graft densities, and the average value of $\epsilon(COO^-)/\epsilon(COOH) = 1.8 \pm 0.3$ was taken for all calculations.

Using the $\epsilon(COO^-)/\epsilon(COOH)$ ratio and the integrals of the absorption band intensities, the degree of dissociation α, i.e., the fraction of deprotonated carboxylic acid groups in comparison to the sum of all carboxylic acid groups, is calculated. In Figure 9, the degree of dissociation α for the four brushes of Figure 7 is shown as a function of the calcium ion concentration. As the

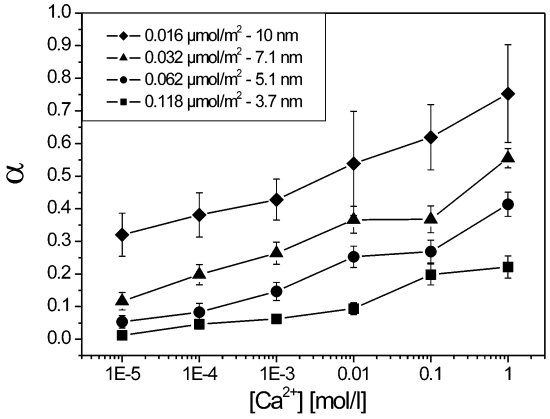

Figure 9. Degree of dissociation α as a function of the calcium ion concentration for the four PMAA brushes of Figure 7. Graft densities of the brushes were 0.118 μmol/m^2 (■), 0.062 μmol/m^2 (●), 0.032 μmol/m^2 (▲), and 0.016 μmol/m^2 (◆).

pH value of the system is neutral, for infinitely high graft densities and infinitely small calcium ion concentrations, almost no dissociation, i.e., $\alpha = 0$, should be expected. This is indeed almost observed for the highest graft density (0.118 μmol/m^2) and the lowest Ca^{2+} concentration (10^{-5} mol/L). The degree of dissociation monotonically increases with increasing calcium ion concentration for all graft densities. All curves show the same general trend but are offset to higher α values for decreasing graft densities. They do not coincide but show an increasing α with decreasing graft density at any given concentration. For example, the brush with the highest graft density is at low calcium ion concentrations practically fully protonated ($\alpha \approx 0.01$ at $[Ca^{2+}] = 10^{-5}$ mol/L), and at 1 mol/L calcium ions approximately 22% of the carboxylic acid groups are deprotonated. In contrast to this, the brush with the lowest graft density is to approximately 32% deprotonated already at the lowest calcium ion concentration. The degree of dissociation increases with increasing calcium ion concentration to $\alpha \approx 0.75$ at $[Ca^{2+}] = 1$ mol/L.

3.5. Influence of the Graft Density. To gain further insight into the influence of the graft density on the complexation of PMAA brushes with metal cations, the series of PMAA brushes with different graft densities of section 3.1 was treated with 0.1 M solutions of $Ca(NO_3)_2$, $Cu(NO_3)_2$, and $Al(NO_3)_3$. To do so, the substrates with the surface-attached brushes were cut into approximately equal pieces, which were then brought into contact with the different metal ion solutions. Hence, the graft densities that were employed for the investigation of the PMAA brush metal ion interaction were almost identical for all three salts. The spectra are displayed in Figure 10 for (a) 0.1 M $Ca(NO_3)_2$, (b) 0.1 M $Cu(NO_3)_2$ and (c) 0.1 M $Al(NO_3)_3$. The graft densities were 0.118, 0.081, 0.062, 0.052, 0.042, 0.032, 0.021, and 0.016 μmol/m^2 from top to bottom. The corresponding anchoring distances were 3.7, 4.4, 5.1, 5.6, 6.2, 7.1, 8.7, and 10 nm. It should be explicitly noted that all samples are well in the brush regime, even at the lowest graft density employed. The transition from the mushroom to the brush regime is generally expected at $D \approx R_g$.[41] For a sodium poly(methacrylate) sample with a weight-averaged molecular weight M_w of 615 000 g/mol, which is much lower than the molecular weight of the surface-attached chains here, Huber et al. have determined in water of pH = 9 a radius of gyration of $R_g = 64.4$ nm.[42]

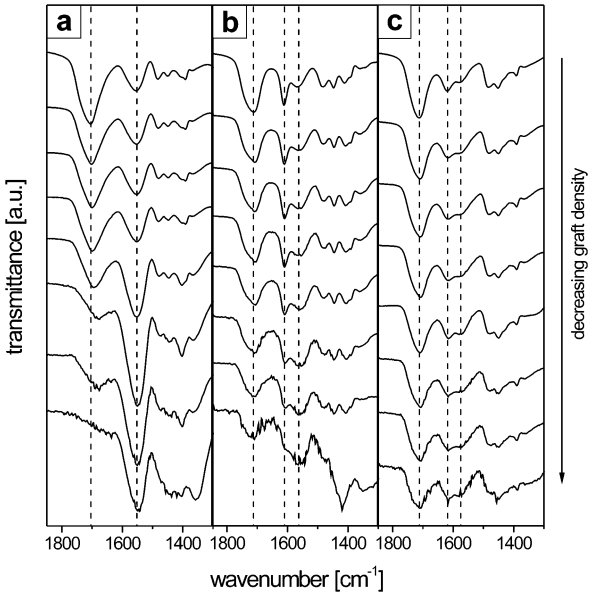

Figure 10. Transmission FTIR spectra (only the carbonyl absorption band region is shown) of PMAA brushes of different graft densities after complexation with (a) 0.1 M $Ca(NO_3)_2$, (b) 0.1 M $Cu(NO_3)_2$, and (c) 0.1 M $Al(NO_3)_3$. The graft densities were 0.118, 0.081, 0.062, 0.052, 0.042, 0.032, 0.021, and 0.016 μmol/m^2 from top to bottom. Peaks corresponding to carboxylic acid and carboxylate vibrational bands are marked with a dashed line.

Accordingly, even for the lowest graft density sample the radius of gyration R_g is much larger than the anchor distance D. A quantitative evaluation of the copper and aluminum ion complexes was not attempted as an unambiguous determination of the extinction coefficients for all carbonyl absorption bands is not feasible from the available data. However, a visual inspection of the spectra allows us to draw some interesting qualitative conclusions. For all three metal ions the general trend that the degree of dissociation increases with decreasing graft density can be derived from the infrared spectra. This can be understood if one considers that the pK_a value of the carboxylic acid groups increases with increasing polymer segment density of the brush. The segment density, however, increases with increasing graft density. A similar observation was made by Kurihara et al.[43] The authors prepared Langmuir−Blodgett films of mixed monolayers of an ionized poly(glutamic acid)-functionalized amphiphile and a monomeric phospholic acid amphiphile in order to obtain polyelectrolyte brushes of different graft densities. After transferring the monolayers to glass plates, infrared spectra showed that the degree of ionization of the carboxylic acid groups decreased with increasing graft density in accordance with our results.

Furthermore, a most interesting behavior can be seen in Figure 10. The peak intensities corresponding to the different complex geometries (e.g., chelating bidentate at 1557 cm^{-1} and bridging bidentate at 1611 cm^{-1} for copper) show a different dependence on the graft density. Similar to the calcium case, the peak intensity due to the formation of chelating bidentate complexes increases with decreasing graft density for copper and aluminum. In contrast to this, in the case of copper, the peak intensity corresponding to the bridging bidentate complex shows a strong absorption already at the highest graft density and increases only slightly with decreasing graft density. This again indicates a stronger

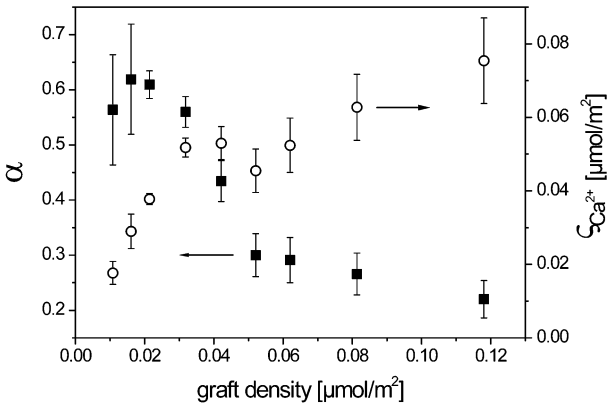

Figure 11. Degree of dissociation α (■) and total adsorbed amount of calcium ions $\varsigma_{Ca^{2+}}$ (○) as a function of the graft density Γ.

complexation of the copper ions in a bridging bidentate coordination in comparison to the chelating bidentate coordination and therefore a less strong dependence of the degree of complex formation on the graft density. In the case of aluminum complexation, the adsorbed amount was generally less and also the dependence on the graft density was weaker. Moreover, the intensities of the bands at 1580 and 1616 cm^{-1} showed an almost similar trend as a function of the graft density. Even though copper and aluminum both were characterized by partially bridging coordination behavior, the exact geometries seem to differ, what is reflected in the stability of the complexes (compare section 3.3) and a difference in the peak position of 23 cm^{-1} (1557 and 1580 cm^{-1}).

Finally, how the calcium complexation depends on the graft density was evaluated quantitatively as described in section 3.4. Figure 11 depicts the degree of dissociation α as a function of the graft density Γ. α is at a maximum at graft densities ≤ 0.03 μmol/m^2 (α ≈ 0.6) and significantly drops between approximately 0.03 and 0.05 μmol/m^2 to a value of α ≈ 0.3. α then further decreases with increasing graft density. At Γ = 0.118 μmol/m^2 a value of α = 0.22 was found. As all brushes are well in the brush regime as discussed above, the observed changes cannot be due to larger structural changes of the surface-attached chains such as a mushroom to brush transition but must be attributed to an increasing self-screening of the carboxylic acid groups with increasing graft density.

An important question with respect to technological applications as well as for the fundamental understanding of the system is how the total amount of calcium ions $\varsigma_{Ca^{2+}}$, i.e., the maximum loading with such ions, depends on the graft density. $\varsigma_{Ca^{2+}}$ is determined by the number of surface-attached monomeric units and the degree of dissociation α. The number of surface-attached monomeric units in turn depends on the graft density Γ and the degree of polymerization, i.e., the number-averaged molecular weight M_n:

$$\varsigma_{Ca^{2+}} = \Gamma \frac{M_n}{M_{MAA}} \alpha \qquad (5)$$

M_{MAA} is the molecular weight of the methacrylic acid repeat unit. On one hand, we have seen that an increasing graft density leads to a decrease in the degree of dissociation due to the self-screening effect. Accordingly, this leads to a decrease in the number of monomeric units taking part in the uptake of calcium ions. On the other hand, however, an increasing graft density means that more monomeric units are incorporated into the brush (compare section 3.1) and should consequently lead to a higher adsorbed amount of the metal ion. The dependence of $\varsigma_{Ca^{2+}}$ on the graft density is included in Figure 11. At low graft densities, between Γ = 0.01 and 0.03 μmol/m^2, where α is almost constant, $\varsigma_{Ca^{2+}}$ increases with increasing Γ as the number of monomeric units of carboxylic acid in the film increases (trivially) linearly with the graft density. However, in the Γ range between Γ = 0.03 and 0.06 μmol/m^2, where α significantly decreases, $\varsigma_{Ca^{2+}}$ becomes approximately constant. In this range, because of the self-screening of the brushes, an increase in the metal loading by increasing the polymer brush graft density is not possible although the brush thickness increases. With further increasing graft density, the change in α becomes less, and hence $\varsigma_{Ca^{2+}}$ seems again to increase, although to a smaller extent than what might be expected if only the increase in thickness was taken into consideration. To elucidate the latter case in more detail, monolayers with even higher graft densities would be required, which is, however, not possible with the current system. This is especially important as at such high graft densities the experimental error in $\varsigma_{Ca^{2+}}$ is rather high.

4. Conclusions

Poly(methacrylic acid) brushes form stable complexes with a variety of metal cations. Infrared spectra reveal different coordination geometries according to the nature of the cation. These lead to great differences in the stability of the complexes; primarily the bridging bidentate coordination shows a greater stability than the chelating bidentate. The graft density, a characteristic parameter of polymer brushes, strongly influences the complexation behavior of weak polyacid brushes. At first, the ratio of carboxylate groups taking part in the different coordination geometries is a function of the graft density. Furthermore, the graft density strongly influences the degree of dissociation and therefore the degree of complexation of the polycarboxylate brush. Finally, the total amount of metal ions that can be adsorbed to the brush is determined by the interplay of two opposing trends: the degree of complexation decreases whereas the number of carboxylic acid units incorporated in the film increases with increasing graft density.

A detailed investigation on the swelling behavior of PMAA brushes in aqueous solutions of mono- and multivalent cations will be the subject of a forthcoming publication.

Acknowledgment. Financial support by the Deutsche Forschungsgemeinschaft, DFG (Schwerpunkt: Polyelektrolyte mit definierter Molekülarchitektur) under Grant Ru 489/6-3 is gratefully acknowledged.

References and Notes

(1) Kazanskii, K. S.; Dubrovskii, S. A. *Adv. Polym. Sci.* **1992**, *104*, 97−133.
(2) Rivas, B. L.; Pereira, E. D.; Moreno-Villoslada, I. *Prog. Polym. Sci.* **2002**, *28*, 173−208.
(3) Balastre, M.; Argillier, J. F.; Allain, C.; Foissy, A. *Colloids Surf., A* **2002**, *211*, 145−56.
(4) McCluskey, P. H.; Snyder, R. L.; Condrate, R. A. *J. Solid State Chem.* **1989**, *83*, 332−9.
(5) Iwasa, K.; Tasaki, I.; Gibbons, R. C. *Science* **1980**, *210*, 338−9.

(6) Tasaki, I.; Byrne, P. M. *Biopolymers* **1994**, *34*, 209−15.
(7) Alexander, S. J. *J. Phys. (Paris)* **1977**, *38*, 983−7.
(8) De Gennes, P. G. *J. Phys. (Paris)* **1976**, *37*, 1445−1452.
(9) De Gennes, P. G. *Macromolecules* **1980**, *13*, 1069−75.
(10) Milner, S. T. *Science* **1991**, *251*, 905−14.
(11) Baltes, H.; Schwendler, M.; Helm, C. A.; Heger, R.; Goedel, W. A. *Macromolecules* **1997**, *30*, 6633−9.
(12) Goedel, W. A.; Luap, C.; Oeser, R.; Lang, P.; Braun, C.; Steitz, R. *Macromolecules* **1999**, *32*, 7599−609.
(13) Halperin, A.; Tirrell, M.; Lodge, T. P. *Adv. Polym. Sci.* **1992**, *100*, 31−71.
(14) Szleifer, I.; Carignano, M. A. *Adv. Chem. Phys.* **1996**, *94*, 165−260.
(15) Stöhr, T.; Rühe, J. *Macromolecules* **2000**, *33*, 4501−11.
(16) Prucker, O.; Rühe, J. *Macromolecules* **1998**, *31*, 592−601.
(17) Prucker, O.; Rühe, J. *Macromolecules* **1998**, *31*, 602−13.
(18) Prucker, O.; Rühe, J. *Langmuir* **1998**, *14*, 6893−8.
(19) Kopf, A.; Baschnagel, J.; Wittmer, J.; Binder, K. *Macromolecules* **1996**, *29*, 1433−41.
(20) Zajac, R.; Chakrabarti, A. *Phys. Rev. E* **1994**, *49*, 3069−78.
(21) Fritz, G.; Schadler, V.; Willenbacher, N.; Wagner, N. J. *Langmuir* **2002**, *18*, 6381−6390.
(22) Raviv, U.; Giasson, S.; Kampf, N.; Gohy, J.-F.; Jerome, R.; Klein, J. *Nature (London)* **2003**, *425*, 163−5.
(23) Biesalski, M.; Rühe, J.; Kügler, R.; Knoll, W. *Handb. Polyelectrolytes Their Appl.* **2002**, *1*, 39−63.
(24) Israels, R.; Leermakers, F. A. M.; Fleer, G. J.; Zhulina, E. B. *Macromolecules* **1994**, *27*, 3249−61.
(25) Israels, R.; Leermakers, F. A. M.; Fleer, G. J. *Macromolecules* **1994**, *27*, 3087−93.
(26) Lyatskaya, Y. V.; Leermakers, F. A. M.; Fleer, G. J.; Zhulina, E. B.; Birshtein, T. M. *Macromolecules* **1995**, *28*, 3562−9.
(27) Zhulina, E. B.; Birshtein, T. M.; Borisov, O. V. *Macromolecules* **1995**, *28*, 1491−9.
(28) Biesalski, M.; Rühe, J. *Macromolecules* **2004**, *37*, 2196−202.
(29) Ballauff, M. *Macromol. Chem. Phys.* **2003**, *204*, 220−34.
(30) Rühe, J.; et al. *Adv. Polym. Sci.* **2004**, *165*, 79−150.
(31) Rühe, J.; Knoll, N. *J. Macromol. Sci., Polym. Rev.* **2002**, *C42*, 91−138.
(32) Biesalski, M.; Johannsmann, D.; Rühe, J. *J. Chem. Phys.* **2002**, *117*, 4988−94.
(33) Guo, X.; Ballauff, M. *Phys. Rev. E* **2001**, *6405*, art. no.-051406.
(34) Zhulina, E. B.; Borisov, O. V.; Birshtein, T. M. *Macromolecules* **1999**, *32*, 8189−96.
(35) Birshtein, T. M.; Zhulina, E. B. *Ber. Bunsen-Ges.* **1996**, *100*, 929−35.
(36) Lazzari, M.; Kitayama, T.; Hatada, K.; Chiantore, O. *Macromolecules* **1998**, *31*, 8075−82.
(37) Deacon, G. B.; Phillips, R. J. *Coord. Chem. Rev.* **1980**, *33*, 227−50.
(38) Yang, L. Q.; Xie, Z. M.; Li, Z. M. *J. Appl. Polym. Sci.* **1997**, *66*, 2457−63.
(39) Nicholson, J. W. *J. Appl. Polym. Sci.* **1998**, *70*, 2353−9.
(40) Nicholson, J. W.; Wasson, E. A.; Wilson, A. D. *Br. Polym. J.* **1988**, *20*, 97−101.
(41) Gennes, P. G. D. *Macromolecules* **1980**, *13*, 1069−75.
(42) Ikeda, Y.; Beer, M.; Schmidt, M.; Huber, K. *Macromolecules* **1998**, *31*, 728−33.
(43) Abe, T.; Hayashi, S.; Higashi, N.; Niwa, M.; Kurihara, K. *Colloids Surf., A* **2000**, *169*, 351−6.

MA049126X